0026-895X/93/060982-07$03.00/0

MOLECULAR PHARMACOLOGY, 43:982-988

DNA Minor Groove Recognition Properties of Pentamidine and its Analogs: A Molecular Modeling Study

PAULETTE A. GREENIDGE,[1] TERENCE C. JENKINS, and STEPHEN NEIDLE

Cancer Research Campaign Biomolecular Structure Unit, The Institute of Cancer Research, Sutton, Surrey, SM2 5NG, UK

Received December 1, 1992; Accepted March 23, 1993

SUMMARY

A molecular mechanics and molecular dynamics approach has been used to examine the structure of the complex formed between pentamidine and the d(CGCGAATTCGCG)$_2$ duplex. Similar energy calculations have also been performed on complexes with closely related pentamidine analogs, using the complex with the parent drug as the starting point. The resulting structures of the drug-DNA complexes and their energetics have been examined and are compared with the reported DNA binding affinities. These studies provide rationalizations for the differences in binding behavior of pentamidine analogs with differing linker chain lengths and aromatic ring substitutions.

The aromatic bis(amidine) compound pentamidine (**1** in Fig. 1) is currently in widespread clinical use for the treatment of PCP in patients with acquired immunodeficiency syndrome (1–3). This opportunistic infection occurs in >70% of such patients and is a major cause of death. However, although pentamidine is a relatively effective treatment, it is associated with a number of toxic side effects. Accordingly, there has been a continuing quest for improved analogs with both diminished toxicity and greater efficacy (4–7).

The precise mode of action of pentamidine is unclear and its major macromolecular targets have not been identified unequivocally, but there is considerable evidence that direct interaction with the pathogenic genome is important (5–8). Biophysical (9, 10) and footprinting studies (11) have shown that the molecule binds to AT-rich regions of duplex DNA. Molecular modeling has suggested (12, 13) that, in common with drugs such as netropsin (14) and berenil (15, 16), it interacts via the minor groove of DNA. We have recently confirmed this prediction by crystallographic and NMR analysis of pentamidine-dodecanucleotide complexes (17, 18).

It has been shown (6, 7) for a series of pentamidine analogs that there is a good correlation between DNA binding affinity, as estimated by stabilization of the DNA helix to coil thermal denaturation transition (T_m), and anti-PCP activity in a rat model. This study examines a representative range of these analogs (compounds **1–7** in Fig. 1) in terms of computed binding energy with a model DNA sequence and structure-activity relationships, using the reported crystallographic structure for the pentamidine-dodecanucleotide complex (17) as a starting point for molecular modeling using combined MM/MD methods.

This work was supported by the Cancer Research Campaign.

[1] Present address: Department of Pharmacy, Federal Institute of Technology, ETH, Zürich, CH-8093, Switzerland.

Methods

Molecular modeling. Initial structures for molecules **1–7** (Fig. 1), with all-*trans* or fully antiperiplanar α,ω-dioxy- or α,ω-diaminoalkane linker functions (13, 17), were constructed using the GEMINI version 1.03 program (19), which was also used for manipulation and interactive docking manoeuvres. All visualizations were carried out on a Silicon Graphics 4D-20G workstation, and calculations were performed using an Alliant FX40/3 computer system.

Atom-centered charges for each molecule were computed from the MNDO wavefunctions (AMPAC, QCPE 506) by the procedure of Orozco and Luque (20), which provides derived MEP charges that closely resemble those obtainable from *ab initio* 6-31G* calculations. However, this method is only applicable to molecules containing ≤50 atoms, and it was thus possible to calculate MEPs only for intact dications **2**, **3**, and **7**. For the remaining ligands MEP charges were computed for symmetry-derived monocationic fragments and subsequently fitted to the entire molecules. Additional AMBER (21) force-field parameters required for the ligands were either derived by interpolation or taken from earlier studies in this laboratory (15, 16, 22). Calculated MEP charges and AMBER force-field parameters are available from the authors upon request.

Initial coordinates for the 12-mer DNA duplex host were taken from the crystal structure of the pentamidine (**1**)-d(CGCGAATTCGCG)$_2$ complex (17) and were used to generate structures of equivalent 1:1 stoichiometry for each DNA-ligand complex. Coordinates for each drug molecule were superimposed, using an RMS overlay fitting procedure, upon those for the reference pentamidine ligand at its crystallographic

ABBREVIATIONS: PCP, *Pneumocystis carinii* pneumonia; MM, molecular mechanics; MD, molecular dynamics; MEP, molecular electrostatic potential; RMS, root mean square; MNDO, moderate neglect of differential overlap.

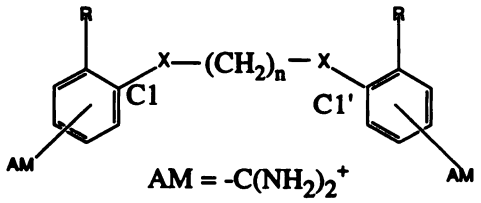

compound	-X-	n	R	amidine ring position
1	O	5	H	para
2	O	4	H	para
3	O	3	H	para
4	O	5	OMe	para
5	NH	5	H	para
6	O	5	H	meta
7	O	4	H	meta

Fig. 1. Structures of the pentamidine analogs.

5′-AATT binding site (17) within the DNA minor groove. Compounds **4–6**, which are essentially isostructural with **1** with respect to the α,ω-disubstituted pentane core, afforded exact overlays and provided equivalent DNA-ligand complexes for subsequent refinement. For the shorter homolog **3**, alternative drug positions were considered by translation of the ligand along the 5′-AATT minor groove tract of the DNA. Thus, the extrema of the binding site for **1** were simulated by overlay of the respective 5′- and 3′-end phenyl rings (with respect to crystal structure definitions), and a model was also constructed for the complex with a centrally positioned **3** ligand. Preliminary calculations for the **3**-DNA complex showed that the model formed by overlap of the 3′-end aromatic residues afforded a superior structure, with an energy difference of ~2 kcal/mol favoring ligand translation towards the 3′ end of the 5′-AATT binding site for **1**.

Alternative complexes were similarly examined for the $n = 4$ ligands, **2** and **7**, to establish the most favorable location of the aromatic residues with respect to the binding site for **1**. The fully extended conformation adopted by these molecules affords two nondegenerate orientations for the distal phenyl groups upon DNA binding. Overlay of either phenyl group with the 5′- or 3′-end aromatic rings of **1** necessarily implies that the residue at the other end of the bound drug is no longer accommodated within the DNA minor groove. Energy calculations for the two situations revealed, in each case, that complexes formed by superimposition of the 3′-phenyl groups are more favorable. In the case of the *meta*-substituted derivatives, **6** and **7**, this situation is further complicated by the distinct conformations available for the ligand molecules, differing in the relative orientation of the amidinium groups with respect to both the ether oxygen atoms and the minor groove (Fig. 2). Models were constructed for each possible drug conformation (Fig. 2) for the **6**-DNA and **7**-DNA complexes and were subjected to MM energy minimization to establish the effect of conformation upon DNA binding. Ranking orders of **6**, A ~ B > C ≈ D, and **7**, A ~ B ≫ C > D, were determined for the ligands, with energy differences spanning ~6 and ~12 kcal/mol, respectively. On this basis, two models (Fig. 2, A and B) for both **6** and **7** were selected for subsequent MD refinement (see below). Energy calculations for alternative complexes with less extended conformations of the drug linker functions confirmed that the all-*trans* extended conformation provides DNA-drug complexes of lower energy.

These procedures were used to establish the optimal position and conformation for each ligand before subsequent refinement. Hydrated sodium cations (23) (i.e., $[Na(H_2O)_6]^+$) were positioned at a phosphorus-sodium distance of 6 Å along the PO_2^- bisector for each DNA phosphate group. The AMBER version 4.0 package (24) was used for all energy calculations.

The DNA-ligand complexes were initially regularized by conjugate-gradient MM to reduce poor intermolecular steric contacts, by using (i) 'belly'-type MM refinement (~300 cycles) to minimize the energy of the bound ligand alone and (ii) MM minimization (~450 cycles) of the unrestrained complex to an RMS energy gradient of ≤0.1 kcal/mol/Å. MD simulations of each complex were subsequently performed for 20 psec (integration time step = 2 fsec) at 300 K. DNA atoms and associated counterions were restrained with a harmonic potential of 5 kcal/mol/Å, and all bonds were constrained using the SHAKE algorithm. Potential energy analysis during MD progress showed that the systems reached equilibrium rapidly, typically at times of ≤2 psec. Atomic coordinates were sampled at 0.2-psec intervals during the simulation period. In each case, the RMS-averaged structure from the accumulated snapshots was subjected to final MM relaxation (<40 cycles), to an RMS energy gradient of ≤0.1 kcal/mol/Å, to generate the refined complex.

Nonbonded energy terms were included up to 8.0 Å (MM) or 9.0 Å (MD). Solvent molecules were not included explicitly; instead, their effect was simulated throughout by the use of a distance-dependent dielectric constant of the form $\epsilon = 4r_{ij}$ (25). Distance restraints corresponding to Watson-Crick base-paired geometry were not included, and no attempt was made to restrain either terminal base pairs or the DNA backbone.

Binding energies are defined as:

$$\Delta E_{bind} = E_{pert}(\text{drug}) + E_{pert}(\text{DNA}) + E_{inter}$$

where ΔE_{bind} is the enthalpy of binding, E_{inter} is the drug-DNA interaction energy, and the E_{pert} terms represent the component perturbation energies for the drug and DNA, relative to the unbound species.

Conformation of the amidinium groups. Recent molecular modeling studies have suggested (7) that the minimum energy conformation for the benzamidine system is one in which the amidinium group is coplanar with respect to the phenyl ring. However, such interplanar torsion results in unfavorable steric clash between the amidinium protons and the *ortho* phenyl ring hydrogens as these atoms approach more closely than their summed van der Waals radii.

Semiempirical AM1 (AMPAC) calculations for the protonated benzamidine cation (Fig. 3) in which the amidinium unit is kept planar indicate that the most favorable torsion angle for rotation about the C(phenyl)-C(amidine) bond is 45°. This conformation reflects a compromise between maximal interplanar π overlap and minimal interproton clash, with a torsional energy barrier of ~4.5 kcal/mol. Further, this rotamer provides an interproton separation of 2.38 Å, which is satisfactorily greater than the summed van der Waals radii for the covalent hydrogen atoms. This conclusion is supported by more extensive *ab initio* quantum mechanical calculations and the crystal structures of **1** and related aromatic amidines (12). The AMBER force-field parameterization used for our study reflects the calculated low torsion energy barrier and provides satisfactory intramolecular H···H separations after minimization; this barrier is lower than that adopted in earlier modeling studies (13, 15, 22).

Results and Discussion

Binding of pentamidine and its analogs. Calculated binding enthalpies and component energies for each minimized complex are collected in Table 1. The ΔE_{bind} values computed for this series span a range of ~9 kcal/mol and reveal trends that correspond to the reported DNA-binding behavior in aqueous solution (6, 7). In particular, the **3** > **1** > **2** order of binding enthalpy computed for the homologous *para* derivatives correlates well with the ranking order of experimental ΔT_m values for these agents and is in broad agreement with the anti-PCP activity *in vivo* (7). Thus, binding of the shorter propamidine homolog **3** is predicted to be more favorable by 1.4 kcal/

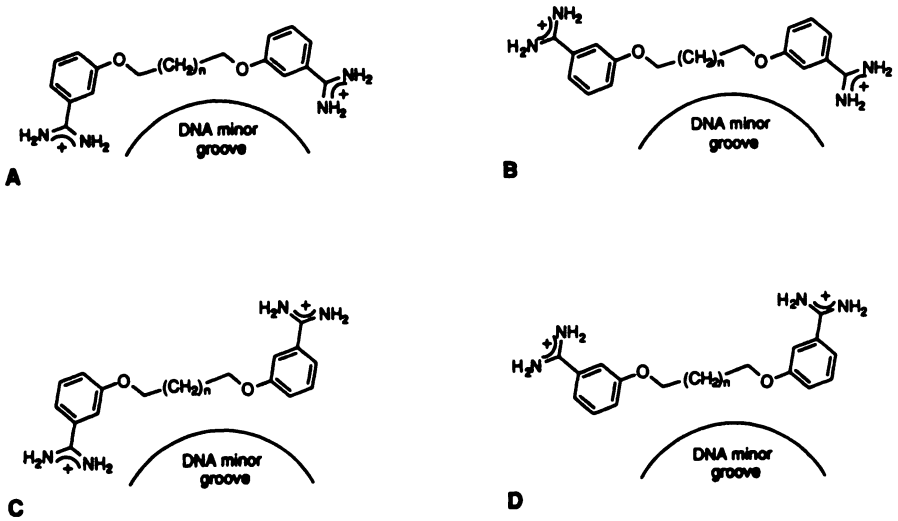

Fig. 2. Effects of conformation for the *meta*-substituted ligands **6** and **7**, showing the four distinct orientations available for the amidinium groups relative to the DNA host and the ether oxygen atoms present in the linker function.

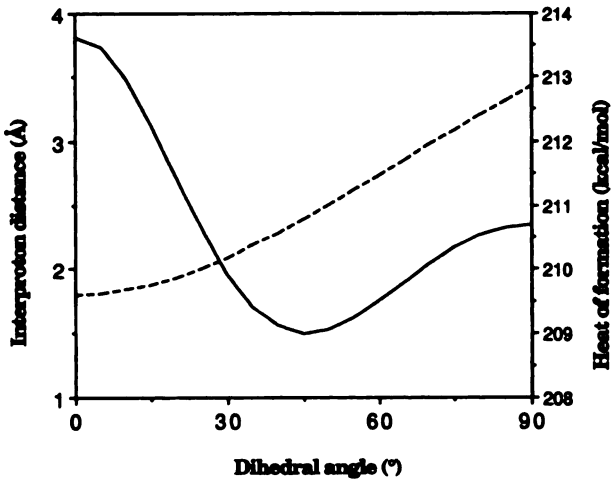

Fig. 3. Dependence of heat of formation (ΔH_f) (——) and H(phenyl)···H(amidinium) separation (– — –) upon interplanar twist, calculated for benzamidine (see text).

mol, relative to the parent $n = 5$ compound, in accord with the greater DNA-binding affinity (Table 1). It is noteworthy that the $n = 4$ homolog **2** gives both the lowest ΔE_{bind} value and the poorest ΔT_m of the *para*-substituted bis(amidine) derivatives **1–5**, as revealed by binding to both double-stranded calf thymus DNA and poly(dA)·poly(dT). This ranking order appears to be dominated by factors involving perturbation of both the DNA and the ligand, rather than specific nonbonded interaction terms. Thus, the **2** > **1** > **3** order for E_{pert}(total) largely predicts the binding affinity for this series, with ligand **2** inducing the greatest level of perturbation (see below). The present study confirms the observation (6, 7) that pentamidine homologs with an odd number (i.e., $n = 3$, 5, etc.) of methylene units in the α,ω-alkanediether linkage are superior DNA-binding ligands, compared with those containing an even number of such moieties.

Ring substitution of the parent compound with methoxy groups results in the binding enthalpy of **4** being >7 kcal/mol more favorable than that of **1**, largely as a consequence of improved nonbonded and electrostatic interaction terms (Table 1). Replacement of the ether moieties in the linker function of **1** with amine residues, to give the equivalent 1,5-diaminopentane derivative **5**, similarly provides slightly more favorable DNA-binding energy. These conclusions agree with the ΔT_m data (Table 1) for the ring-functionalized and linker-modified bis(amidine) compounds, **4** and **5**, respectively.

However, the correlation between the predicted DNA-binding affinity and experimental T_m data is less conclusive for the isomeric bis(amidine) pairs, i.e., **1/6** and **2/7**, that differ solely in the ring position of the charged amidinium substituents. The computed ΔE_{bind} values predict that the *meta*-substituted isomers should be of higher affinity, largely due to superior electrostatic or hydrogen-bonded interactions (see below), whereas the solution data (Table 1) suggest that binding to calf thymus DNA and poly(dA)·poly(dT) is weaker, particularly in the case of the synthetic polynucleotide. Interestingly, this study nevertheless confirms the ranking order determined for the *meta*-substituted isomers (Table 1), whereby ligands with an even number of methylene units in the diether linkage bind more effectively to DNA (7) than do homologs containing odd numbers of such units.

TABLE 1

Calculated energies for interaction of bis(amidine) compounds with d(CGCGAATTCGCG)$_2$ and comparison with thermal denaturation data

All energies were calculated using the AMBER force-field (21). DNA numbering system used was as follows:

```
5′-C1  G2  C3  G4  A5  A6  T7  T8  C9  G10 C11 G12
   G24 C23 G22 C21 T20 T19 A18 A17 G16 C15 G14 C13-5′
```

Thermal denaturation data were taken from the study of Corey *et al.* (7), where $\Delta T_m = T_m$(DNA-drug complex) – T_m(DNA alone). CT-DNA and (dA)·(dT) refer to calf thymus DNA and poly(dA)·poly(dT), respectively. E_{NB} and E_q represent the nonbonded and electrostatic energy components, respectively, of the interaction enthalpy.

Ligand	ΔE_{bind}	E_{inter}		E_{pert}		ΔT_m/°C	
		E_{NB}	E_q	Drug	DNA	CT-DNA	(dA)·(dT)
	kcal/mol	kcal/mol		kcal/mol			
1	−65.5	−42.4	−27.4	0.6	3.7	10.7 ± 0.6	22.9 ± 0.7
2	−63.4	−40.4	−28.0	1.2	3.8	8.3 ± 2.5	17.9 ± 1.6
3	−66.9	−41.2	−26.5	0.0	0.9	14.7 ± 1.7	32.0 ± 0.7
4	−72.5	−48.2	−28.5	2.5	1.7	12.0 ± 0.7	27.2 ± 0.1
5	−67.0	−44.4	−27.7	3.3	1.8	11.3 ± 0.2	20.7 ± 0.3
6A	−66.6	−44.1	−28.3	0.8	5.1	7.6 ± 0.6	7.6 ± 1.5
6B	−67.7	−41.4	−30.1	1.3	2.5	7.6 ± 0.6	7.6 ± 1.5
7A	−67.9	−42.3	−29.6	0.6	3.4	8.1 ± 0.6	15.2 ± 1.4
7B	−69.5	−42.6	−27.9	1.0	0.0	8.1 ± 0.6	15.2 ± 1.4

The discrepancy for isomeric ligand pairs may, in part, reflect the exclusion of solvation effects from our energy calculations. This conclusion is supported by the observation that only energies for closely isostructural ligands appear to correlate with the experimental data, suggesting that entropic and/or solvation factors may differ for the *para*- and *meta*-substituted series of agents. The roles of entropic and enthalpic contributions to binding have been discussed for binding of netropsin to the analogous d(GCGAATTCGC)$_2$ duplex (26).

Analysis of close nonbonded contacts (i.e., atomic separations of ≤3 Å) between the DNA and ligands **1–7** reveals that the energy contribution to the interaction from the linker moiety is broadly independent of chain length and complexation. However, atomic contacts involving the phenyl groups of the drugs give a good correlation with the computed nonbonded interaction energy (E_{NB} in Table 1), suggesting that binding is dominated by interaction between the aromatic residues and the DNA. We note that isomeric pairs **1/6** and **2/7** make similar numbers of close contacts with the DNA host via these residues, in accord with the suggestion that *meta*-substituted ligands afford superior electrostatic interaction. Although the hydrogen bond energy is mainly reflected in the electrostatic component, the AMBER force field used includes an explicit hydrogen bond 10–12 term (21, 24). This hydrogen bond energy is included in the E_{NB} term (Table 1). Only in the case of **6** and **7** does this term become significant, with values of −1.7 and −1.4 kcal/mol, respectively, contrasting with an average value of −0.4 kcal/mol for the **1–5** analogs.

Details of pentamidine groove-binding interaction. The structure for the minimized **1**-d(CGCGAATTCGCG)$_2$ complex (not shown) has the drug molecule located within the A5-T8 tract of the DNA, such that the center of the molecule is displaced by ~0.3 base pairs relative to the diad axis of the DNA. In accord with crystallographic, solution NMR, and footprinting studies (11, 17, 18), pentamidine occupies a 4-base pair 5′-AATT site, although the 3′-end phenyl ring is displaced relative to the crystal structure. The polymethylene linker retains an extended conformation with a C1···C1′ chain length of 9.70 Å, compared with 9.13 and 9.75 Å in the crystal structures of the complex (17) and free drug (12), respectively. Further, the phenyl groups are aligned to be parallel to the walls of the minor groove and the amidinium groups are twisted out of the planes of the phenyl rings, by 13° and 20° at the 5′ and 3′ ends, respectively. These conformational features were common for ligands **1–7** after MD refinement of the complexes, with retention of the extended, all-*trans* geometries and amidinium torsion angles of 17 ± 5°.

In contrast to the crystal structure for the pentamidine-oligomer complex, we find that the model has no explicit hydrogen-bonded contacts (<3 Å) with base acceptors at the floor of the DNA minor groove. This behavior is due to displacement of the drug relative to the crystal structure position and the more extended conformation adopted by the ligand (see above). Indeed, the closest (amidine)N···DNA base contacts are >4 Å for interaction with both N3(A5) and N3(A17), rather than the values of 2.81 and 2.94 Å, respectively, found in the crystal structure. However, the model for **1** shows weak contacts, via the amidinium group, with the deoxyribose oxygen atoms, with (amidine)N···O4′(A6/A18) separations of 3.66 and 3.44 Å, respectively. Equivalent hydrogen bonds are also seen in the crystal structure but are considerably stronger at separations of ~2.8 Å. The oxygen atoms in the diether linkage of **1** make no direct contacts with the DNA, in accord with the crystal structure (17). In the modeled complex, therefore, hydrogen-bonded interactions do not play as dominant a role in ligand positioning as is found in crystallographic and NMR studies (17, 18).

The energy-refined structure has a RMS deviation of only 0.6 Å with respect to the crystal structure, and induced widening of the minor groove is evident in the drug-bound region, compared with the native DNA crystal structure (27). Indeed, induced opening of the A5-C9 minor groove tract is apparent for all the drugs studied, confirming the suggestion of drug 'clamping' by the DNA (17) and, hence, suggesting that increased van der Waals factors may be involved. The minor groove is mostly unchanged in width for representative drug-DNA complexes (Fig. 4), as determined by either P···P or H4′···H5′ interstrand separations (28), compared with the crystal structure for the **1**-DNA complex (Fig. 4), but is opened by ~0.5–1 Å in comparison with the native DNA duplex (27).

Details of groove-binding interaction for the analogs. The structure for the minimized **2**-d(CGCGAATTCGCG)$_2$ complex shows that the drug retains the close contacts of **1** at

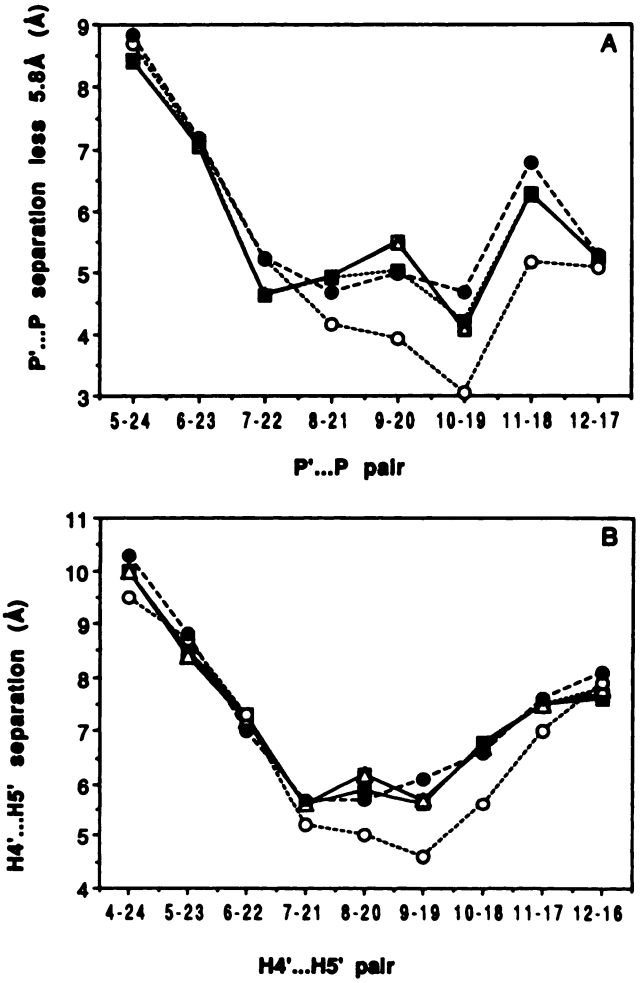

Fig. 4. Plots of minor groove width in terms of interstrand separation for the native dodecamer (○) and its crystal complex with **1** (●), together with the MD-refined complexes formed with analogs **1** (□), **3** (■), and **4** (△). A, Interstrand P···P distances. B, Interstrand H4′···H5′ and H5′···H4′ distances between atoms of a residue on one strand and the (*n*+3)th residue on the second strand.

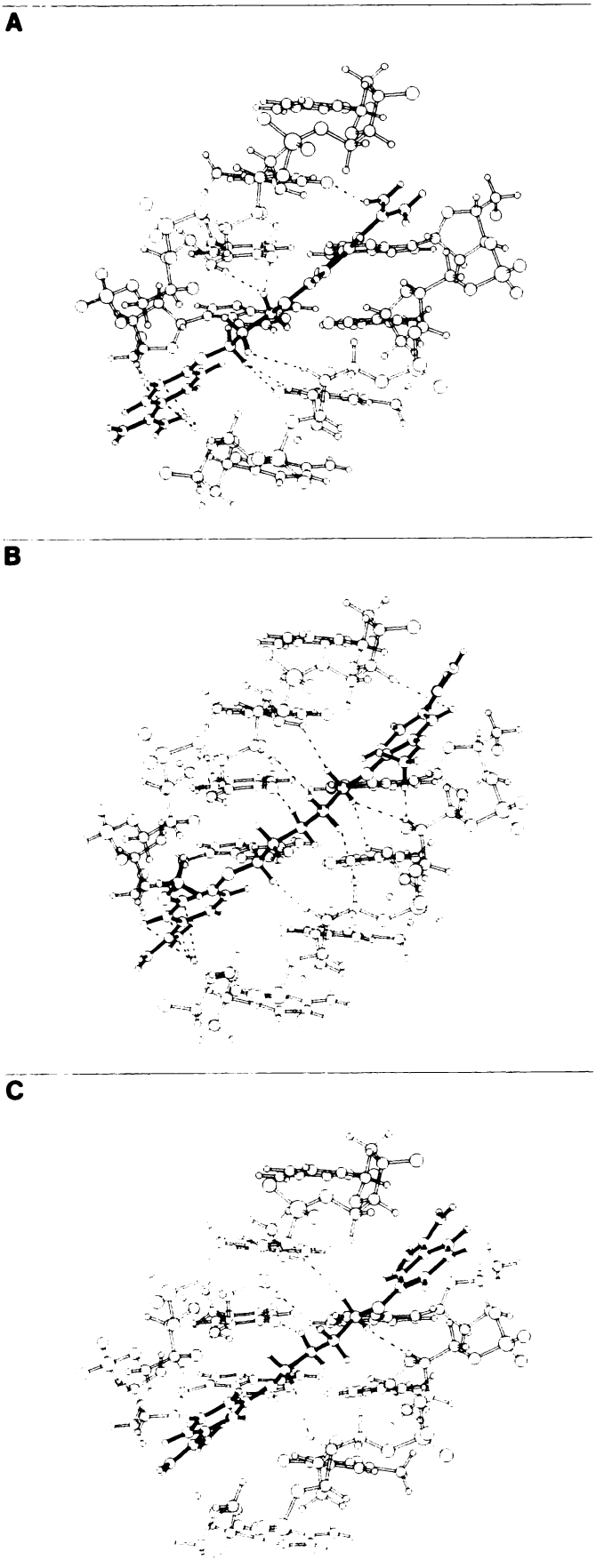

the 3′ end of the AT-rich tract but that nonbonded contacts with the DNA are lost at the 5′ end of the binding site because of the conformation necessarily adopted by the shorter linker function. Inspection of conformers for **2** other than the favored all-*trans* structure showed that binding energies were ≥10 kcal/mol poorer when the conformers were bound to DNA, although this perturbation reduces to only ~1 kcal/mol for rotamers of the free ligands. This conformational dependence, together with energetically favored retention of all-*trans* geometry, explains why *para*-substituted homologs with an odd number of CH_2 units in the polymethylene linkage are superior DNA-binding molecules, compared with those that contain an even number.

The refined structure for the **3**-oligomer complex (Fig. 5A) shows that the drug occupies a noncentrosymmetric site that spans 1 fewer base pairs than **1** (in accord with its shorter length), to give an effective 3-base pair 5′-ATT binding site or recognition sequence. The molecule makes a snug fit to the floor of the minor groove and is bound via a strong hydrogen bond at the 5′ end of this site to a thymine base, with an (amidine)N···O2(T20) separation of 3.20 Å. The close fit favors increased nonbonded interactions with the DNA, without inducing perturbation of the duplex (Table 1; Fig. 5A), suggesting that the molecule is more closely isohelical with the minor groove of the DNA than is pentamidine itself. This conclusion is supported by the averaged radial distance of the inner-facing phenyl carbon atoms of the ligands (i.e., C2, C3, C2′, and C3′ in Fig. 6) from the mean helical axis of the DNA being 6.8 and 6.7 Å for **1** and **3**, respectively. These factors result in the shorter homolog being accommodated more deeply in the groove, in accord with superior DNA-binding activity for **3**.

The ring- and linker-modified analogs, **4** and **5**, respectively, form centrosymmetric 4-base pair complexes with the ligands displaced towards the 3′ end of the 5′-AATT binding site by ~0.5 base pair, relative to the parent molecule **1**. This displacement facilitates increased van der Waals contacts with the walls of the minor groove and results in strong hydrogen-bonded contact with deoxyribose oxygen acceptors, with (amidine)N···O4′(A6/A18) separations of 3.09/3.07 and 3.34/3.33 Å for **4** and **5**, respectively. Additional hydrogen-bonded contacts, at distances of 3.52 and 3.35 Å, respectively, are made via O3′(C9); ligand **5** forms an additional (amidine)N···O3′(A18) hydrogen bond, at a 3.33-Å separation. Fig. 5B shows the **4**-oligomer complex after refinement. Interestingly, neither **4** nor **5** is able to make strong hydrogen-bonded contacts with base acceptors located at the floor of the minor groove. Compound **4** nevertheless makes closer contacts with N3(A5) and N3(A17) than does **1**, at distances of 3.49 and 3.75 Å, respectively. Hydrogen bonds are not formed with the amine moieties of the α,ω-diaminopentane ligand **5**.

The *meta*-substituted ligands **6** and **7**, form effectively centrosymmetric complexes, with DNA base sequence preferences that resemble those of their isomers, **1** and **2**. In contrast to the *para*-substituted counterparts, however, the *meta*-functionalized ligands (i.e., models **6A** and **7A**; see Fig. 2A) achieve explicit, close, hydrogen-bonded contacts with the DNA bases, rather than their associated sugar residues. Thus, contacts are

Fig. 5. Views of the low energy complexes formed between the DNA and the pentamidine analogs, after MD refinement, showing close drug-DNA contacts. A, **3**; B, **4**; C, **7A**. Ligand molecules shown in dark.

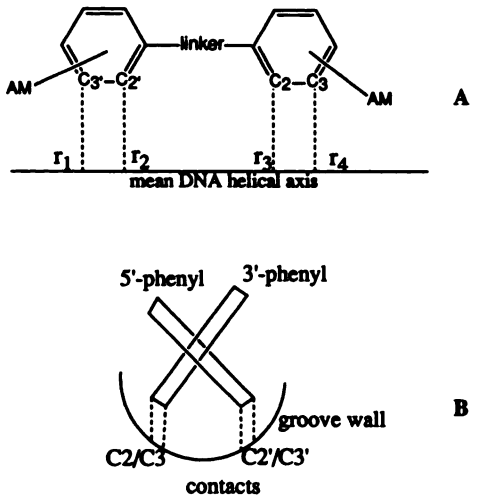

Fig. 6. C2/C3 and C2′/C3′ ligand-DNA minor groove contacts. A, Schematic diagram of the radial distance of the inner-facing phenyl carbon atoms of the ligand from the mean DNA helical axis. B, Schematic view along the minor groove looking from the 3′ end, showing contact with the groove wall. Mean radial distance = $(r_1 + r_2 + r_3 + r_4)/4$.

formed between the amidinium donors of **6** and adenine acceptors within the A6-T8 base tract, with (amidine)N···N3(A6/A17/A18) separations of 2.84, 3.11, and 3.00 Å, respectively, and with subtended NH···N angles of ~150°. Close contacts are not formed with either O4′ or O3′ acceptor atoms on the sugars. The shorter homolog, **7** (Fig. 5C), also forms strong hydrogen-bonded contacts with the adenine bases, with (amidine)N···N3(A5/A6/A18) separations of 3.18, 3.17, and 2.97 Å, respectively. These superior contacts are reflected in the electrostatic interaction energies determined for the *meta*- and *para*-substituted analogs (Table 1).

Examination of the conformations available for the *meta*-substituted ligands reveals that a second binding mode is feasible (Fig. 2B), which facilitates simultaneous interaction with the phosphate backbone of the DNA at the 3′ end of the binding site (i.e., models **6B** and **7B**), although superior binding is again afforded by the $n = 4$ homolog (Table 1). The base sequence preferences for these conformations do not differ significantly from those for the **6A** and **7A** counterparts, although the pattern of hydrogen bonding is altered. Thus, (amidine)N···O2(T20) contacts of 2.80 and 2.93 Å (subtended NH···N angles of ~145°) are achieved at the 5′ end of the site for **6B** and **7B**, respectively. Close contacts are made with the C9pG10 phosphate oxygen at the 3′ end, with (amidine)N···O2P separations of 2.75 and 2.85 Å, respectively, and with subtended NH···O angles of ~120°. Our calculations indicate that the B-type extended ligand conformation induces lower perturbation of both the DNA and the drug (Table 1), particularly in the case of the shorter molecule **7**. However, the binding enthalpy differences computed for these conformers are not reflected in nonbonded or electrostatic energy components and may possibly result from the exclusion of explicit solvent molecules from our calculations.

The refined **7**A-DNA complex (Fig. 5C) indicates that *meta* orientation of the amidinium groups facilitates effective penetration of the DNA minor groove for homologs containing even numbers of methylene groups. This feature is reflected in superior binding enthalpy for **7** relative to **2** (Table 1) and contrasts with the ranking order determined for the *para*-substituted compounds. This conclusion is supported by the mean radial distance of the inner-facing phenyl carbon atoms from the mean DNA helical axis (Fig. 6) being ~7.7 and ~7.3 Å for **6** and **7**, respectively. These distances are significantly greater than those achieved by the equivalent *para*-substituted analogs (see earlier), indicating that derivatives with poor binding energy and lower ΔT_m values are accommodated less snugly within the DNA minor groove.

Conclusions

Our combined MM/MD approach, using the $d(CGCGAATTCGCG)_2$ duplex as a model DNA host, provides a qualitative method to compare the binding properties of pentamidine and its analogs. The calculated binding enthalpies predict a ranking order for interaction that agrees with available solution DNA-binding data, at least for structurally similar compounds.

For pentamidine itself, this procedure results in a drug conformation that is closely related, but not identical, to that in the crystal structure complex (17). Dynamic simulation results in a more extended molecule that makes rather different hydrogen-bonded and nonbonded contacts with the minor groove of the DNA host. However, in view of the 2.1-Å crystallographic resolution and the high temperature factors associated with the bound ligand (17), particularly at the 5′ end of the binding site, these structural differences are unlikely to be significant. It is also possible that the models may be improved by the inclusion of explicit solvent in the MD calculations, because in the crystal structure water molecules are located in the minor groove vicinity of the bound drug. However, such simulations would be computationally expensive for series of compounds. The satisfactory correspondence achieved for computed and experimental binding data using the protocol adopted in this study suggests that more extended calculations are probably not justified.

We predict that *para*-substituted bis(amidine) compounds with an odd number of methylene units in the linker, but *meta*-substituted analogs containing an even number of such units, are effectively more isohelical with the DNA minor groove. The superior DNA-binding afforded by these structural requirements results from more effective penetration of the minor groove and reduced perturbation factors. These conclusions are in broad agreement with estimated radii of curvature for these agents (7), although we note that such calculations are less satisfactory for the *meta*-substituted compounds. However, modeling suggests that the positional isomers achieve rather different patterns of hydrogen-bonded interaction with the DNA minor groove. In conclusion, our calculations provide a basis for the rational design of improved DNA-binding agents of this class, with potential anti-PCP activity.

Acknowledgments

We are grateful to Prof. R. E. Dickerson for the NEWHEL91 program and to Dr. M. Orozco for the MEP program. We also thank Drs. K. Edwards and C. Laughton of this unit for valuable discussions.

References

1. Montgomery, A. B., J. M. Luce, J. Turner, E. T. Lin, R. J. Debs, K. J. Corkery, E. N. Brunette, and P. C. Hopewell. Aerosolised pentamidine as sole therapy for *Pneumocystis carinii* pneumonia in patients with acquired immunodeficiency syndrome. *Lancet* **2**:480–482 (1987).
2. Gazzard, B. G. *Pneumocystis carinii* pneumonia and its treatment in patients with AIDS. *J. Antimicrob. Chemother.* **23**:67–75 (1989).
3. Wispelwey, B., and R. D. Pearson. Pentamidine: a review. *Infect. Control Hosp. Epidemiol.* **12**:375–381 (1991).

4. Walzer, P. D., C. K. Kim, J. Foy, M. J. Linke, and M. Cushion. Cationic antitrypanosomal and other antimicrobial agents in the therapy of experimental *Pneumocystis carinii* pneumonia. *Antimicrob. Agents Chemother.* **32**:896–905 (1988).
5. Jones, S. K., J. E. Hall, M. A. Allen, S. D. Morrison, K. A. Ohemeng, V. V. Reddy, J. D. Geratz, and R. R. Tidwell. Pentamidine analogs in the treatment of experimental *Pneumocystis carinii* pneumonia. *Antimicrob. Agents Chemother.* **34**:1026–1030 (1990).
6. Tidwell, R. R., S. K. Jones, J. D. Geratz, K. A. Ohemeng, M. Cory, and J. E. Hall. Analogues of 1,5-bis(4-amidinophenoxy)pentane (pentamidine) in the treatment of experimental *Pneumocystis carinii* pneumonia. *J. Med. Chem.* **33**:1252–1257 (1990).
7. Cory, M., R. R. Tidwell, and T. A. Fairley. Structure and DNA binding activity of analogues of 1,5-bis(4-amidinophenoxy)pentane (pentamidine). *J. Med. Chem.* **35**:431–438 (1992).
8. Shapiro, T. A., and P. T. Englund. Selective cleavage of kinetoplast DNA minicircles promoted by antityrypanosomal drugs. *Proc. Natl. Acad. Sci. USA* **87**:950–954 (1990).
9. Zimmer, C., and U. Wähnert. Non-intercalating DNA-binding ligands: specificity of the interaction and their use as tools in biophysical, biochemical and biological investigations of the genetic material. *Prog. Biophys. Mol. Biol.* **47**:31–112 (1986).
10. Luck, G., C. Zimmer, and D. Schweizer. DNA binding studies of the nonintercalative ligand pentamidine: dA·dT base-pair preference. *Stud. Biophys.* **125**:107–119 (1988).
11. Fox, K. R., C. E. Sansom, and M. F. G. Stevens. Footprinting studies on the sequence-selective binding of pentamidine to DNA. *FEBS Lett.* **266**:150–154 (1990).
12. Lowe, P. R., C. E. Sansom, C. H. Schwalbe, and M. F. G. Stevens. Crystal structure and molecular modelling of the antimicrobial drug pentamidine. *J. Chem. Soc. Chem. Commun.* 1164–1165 (1989).
13. Sansom, C. E., C. A. Laughton, S. Neidle, C. H. Schwalbe, and M. F. G. Stevens. Structural studies on bio-active compounds. XIV. Molecular modelling of the interactions between pentamidine and DNA. *Anti-Cancer Drug Design* **5**:243–248 (1990).
14. Kopka, M. L., C. Yoon, D. Goodsell, P. Pjura, and R. E. Dickerson. Binding of an antitumour drug to DNA: netropsin and CGCGAATTBrCGCG. *J. Mol. Biol.* **183**:553–563 (1985).
15. Brown, D. G., M. R. Sanderson, J. V. Skelly, T. C. Jenkins, T. Brown, E. Garman, D. I. Stuart, and S. Neidle. Crystal structure of a berenil-dodecanucleotide complex: the role of water in sequence-specific ligand binding. *EMBO J.* **9**:1329–1334 (1990).
16. Lane, A. N., T. C. Jenkins, T. Brown, and S. Neidle. Interaction of berenil with the *Eco*RI dodecamer d(CGCGAATTCGCG)$_2$ in solution studied by NMR. *Biochemistry* **30**:1372–1385 (1991).
17. Edwards, K. J., T. C. Jenkins, and S. Neidle. Crystal structure of a pentamidine-oligonucleotide complex: implications for DNA-binding properties. *Biochemistry* **31**:7104–7109 (1992).
18. Jenkins, T. C., A. N. Lane, S. Neidle, and D. G. Brown. NMR and molecular modeling studies of the interaction of berenil and pentamidine with d(CGCAAATTTGCG)$_2$. *Eur. J. Biochem.* **213**:1175–1184 (1993).
19. Beveridge, A. J. GEMINI version 1.03 molecular modeling package. CRC Biomolecular Structure Unit, The Institute of Cancer Research, Sutton, Surrey, SM2 5NG, UK. (1991).
20. Orozco, M., and F. J. Luque. On the use of AM1 and MNDO wavefunctions to compute accurate electrostatic charges. *J. Comput. Chem.* **11**:909–923 (1990).
21. Weiner, S. J., P. A. Kollman, D. A. Case, U. C. Singh, C. Ghio, G. Alagano, S. Profeta, and P. Weiner. A new force-field for molecular mechanical simulation of nucleic acids and proteins. *J. Am. Chem. Soc.* **106**:765–784 (1984).
22. Laughton, C. A., T. C. Jenkins, K. R. Fox, and S. Neidle. Interaction of berenil with the *tyr*T DNA sequence studied by footprinting and molecular modelling: implications for the design of sequence-specific DNA recognition agents. *Nucleic Acids Res.* **18**:4479–4488 (1990).
23. Singh, U. C., S. J. Weiner, and P. Kollman. Molecular dynamics simulations of d(C-G-C-G-A)·d(T-C-G-C-G) with and without 'hydrated' counterions. *Proc. Natl. Acad. Sci. USA* **82**:755–759 (1985).
24. Pearlman, D. A., D. A. Case, J. C. Caldwell, G. L. Seibel, U. C. Singh, P. Weiner, and P. A. Kollman. AMBER version 4.0. University of California, San Francisco (1991).
25. Orozco, M., C. A. Laughton, P. Herzyk, and S. Neidle. Molecular modelling of drug-DNA structures: the effects of differing dielectric treatment on helix parameters and comparison with a fully solvated structural model. *J. Biomol. Struct. Dyn.* **8**:359–373 (1990).
26. Marky, L., and K. J. Breslauer. Origins of netropsin binding affinity and specificity: correlations of thermodynamic and structural data. *Proc. Natl. Acad. Sci. USA* **84**:4359–4363 (1987).
27. Drew, H. R., and R. E. Dickerson. Structure of a B-DNA dodecamer. III. Geometry of hydration. *J. Mol. Biol.* **151**:535–556 (1981).
28. Neidle, S. Minor-groove width and accessibility in B-DNA drug and protein complexes. *FEBS Lett.* **298**:97–99 (1992).

Send reprint requests to: Terence C. Jenkins, Cancer Research Campaign Biomolecular Structure Unit, The Institute of Cancer Research, Sutton, Surrey, SM2 5NG, UK.